J Mater Sci (2009) 44:6273–6279
DOI 10.1007/s10853-009-3860-6

Hydrothermal synthesis of calcium hydroxyapatite nanorods in the presence of PVP

Xingwei Du · Ying Chu · Shuangxi Xing · Lihong Dong

Received: 3 April 2009 / Accepted: 29 August 2009 / Published online: 17 September 2009

Abstract Calcium hydroxyphosphate ($Ca_{10}(PO_4)_6(OH)_2$, HAP) nanorods have been successfully synthesized by a simple and mild hydrothermal treatment in the presence of polyvinylpyrrolidone (PVP). A complex of calcium nitrate ($Ca(NO_3)_2$) and Na_2HPO_4 was used to supply the calcium and phosphate ions during the reactions. The synthesis of pure HAP nanorods was under near neutral condition. The morphology and structure of the samples were characterized by transmission electron microscope (TEM), scanning electron microscope (SEM), X-ray diffraction (XRD), and Fourier transform infrared (FT-IR) spectroscopy analysis. The nanorods were uniform with diameter of 20–25 nm and length ranging from several hundreds of nanometers to several micrometers. The influence of different experiment conditions, i.e., the PVP concentration, molar ratio of Ca^{2+} to HPO_4^{2-}, reaction time, and temperature, on the morphology of the nanorods was investigated. The formation mechanism of rod-like HAP and effects of PVP on the crystal nucleation and growth have also been discussed.

Introduction

One dimensional inorganic nanomaterials, such as nanotubes, nanowires, nanobelts, and nanorods, have recently attracted much attention because of their potential applications in electronics, optoelectronics, and memory devices [1–3]. In the past decade, template methods including porous alumina polycarbonate membranes, carbon nanotubes, microemulsions, and aqueous surfactant media by using a seeded growth process have been used for the synthesis of one dimensional nanocrystals [4–7]. Among the methods mentioned above, surfactant-based templating systems show great promise in obtaining nanocrystalline material because of their high efficiency in controlling the particle morphology [8–10].

Among inorganic nanomaterials, calcium phosphates (CaP) are the most ubiquitous family of bioceramics, which are well known for their use in biological applications. Owing to their chemical and structural similarity to the mineral part of bones, several forms of CaP especially bioactive ones, such as calcium hydroxyphosphate (HAP), are used as substitute materials for bones in orthopedic, dental, and maxillofacial applications [11, 12]. In addition, HAP can be used as drug delivery agent, delivering anti-tumor agents and antibodies in the treatment of osteomyelitis that is often treated by excision of necrotic tissue and irrigation of the wound [13]. Potential usage of HAP as a protein delivery agent was also examined [14]. These promising applications have driven the development for various methods to synthesize HAP nanostructures. Somiya's group has pioneered the hydrothermal synthesis of single crystal hydroxyapatite [15, 16]. Ahn et al. [17] reported nanostructure synthesis of hydroxyapatite-based bioceramic in the presence of yttria stabilized zirconia, prepared by chemical precipitation. Wu and Bose [18] used template system to synthesize hydroxyapatite nanocrystalline with high surface area and little agglomerated porous morphology, where mono-dodecyl phosphate ($((C_{12}H_{25}O)P(O)(OH)_2$) was used as the surfactant. Koutsoukos et al. [19], on the other hand, prepared hydroxyapatite nanocrystalline from simulated milk ultrafiltrate (SMUF) solutions. Calcium phosphate nanofilaments with different lengths and widths were synthesized in reverse micelles by Mann et al. [20]. Rod-shaped HAP powder is highly preferred in most of the research as motivated by

X. Du · Y. Chu (✉) · S. Xing · L. Dong
Department of Chemistry, Northeast Normal University, Changchun, Jilin 130024, People's Republic of China
e-mail: chuying@nenu.edu.cn

imitating the microstructure of teeth. In other words, rod-like nano-HAP powder is believed to be the most favorable "building block "to construct dental material, for example, successful synthesis of the mesoporous hydroxyapatite using cationic surfactant as template through a hydrothermal method [21] and preparation of ultrahigh-aspect-ratio hydroxyapatite nanofibers in reverse micelles under hydrothermal conditions [22]. However, strict reaction conditions or complicated instrumentation in the aforesaid methods are involved. For this reason, it is of great importance to develop inexpensive HAP synthesis methods to control the crystal morphology and grain size. In this paper, we report a simple and mild hydrothermal route to synthesize stable hexagonal HAP nanorods. The surface-regulating polymer PVP is used as a capping agent to regulate the nucleation and crystal growth of HAP crystal. The formation mechanism of rod-like HAP and effects of PVP on the crystal nucleation and growth have also been discussed.

Experimental details

Materials

All of the reagents were analytical grade and used without any further purification. $Na_2HPO_4{\cdot}12H_2O$, $Ca(NO_3)_2{\cdot}4H_2O$, ethanol, and polyvinylpyrrolidone (PVP, 30000 g mol^{-1}) were purchased from Shanghai Sinopharm Chemical Reagent Co. Ltd.

Preparation of HAP nanorods

The synthesis of pure calcium hydroxyphosphate was based on the following reaction:

$$6Na_2HPO_4 + 10Ca(NO_3)_2 + 2H_2O \rightarrow Ca_{10}(PO_4)_6(OH)_2 + 12NaNO_3 + 8HNO_3$$

In a typical synthesis, two identical solutions were prepared by dissolving 0.15 g of PVP in 20 mL of distilled water (the concentration of PVP was 2.5×10^{-4} mol L^{-1}). Then, 0.708 g of $Ca(NO_3)_2{\cdot}4H_2O$ and 0.716 g of $Na_2HPO_4{\cdot}12H_2O$ were added into one of the two solutions, respectively. The two solutions as-obtained were mixed together and stirred for 30 min, the mixture was then transferred into a 50 mL stainless Teflon-lined autoclave and heated at 180 °C for 24 h. The resulting suspension was naturally cooled to room temperature, and washed with distilled water and ethanol several times. Finally, the samples were dried at 50 °C for 12 h. Further experiments, in which the the PVP concentration, molar ratio of Ca^{2+} to HPO_4^{2-}, reaction time, and temperature were varied, were also conducted to determine the roles of the surfactant PVP, the concentration of reactants, the temperature, and time.

The influence of different experiment conditions, i.e., the PVP concentration, molar ratio of Ca^{2+} to HPO_4^{2-}, reaction time, and temperature, on the morphology of the nanorods was investigated.

Characterization

The crystallinity and phase purity of the products were examined by powder X-ray diffraction (XRD) on Rigaku D/max 2500V PC diffractometer with Cu-Kα radiation. The morphologies and microstructures of the as-synthesized samples were investigated by transmission electron microscope (TEM, JEOL 2010, and Hitachi Model H-800), scanning electron microscope (SEM, JEOL FESEM JEM-6700F), and energy dispersive spectrometer (EDS, JEOL 2010) attachment. Fourier transform infrared (FT-IR) spectroscopy analysis was carried out on a Magna FT-IR 760 spectrophotometer.

Results and discussion

The XRD pattern of the HAP nanorods as-synthesized shows characteristic peaks of phase-pure HAP crystalline structure, which is consistent with the standard database (1997, JCPDS 73-1731) (Fig. 1a). Furthermore, all diffraction peaks can be indexed to the hexagonal HAP unit cell with lattice constant $a = b = 0.9400$ nm, and $c = 0.6930$ nm. Despite being calcined in a furnace at 800 °C, the XRD pattern of the HAP nanorods remains unchanged,

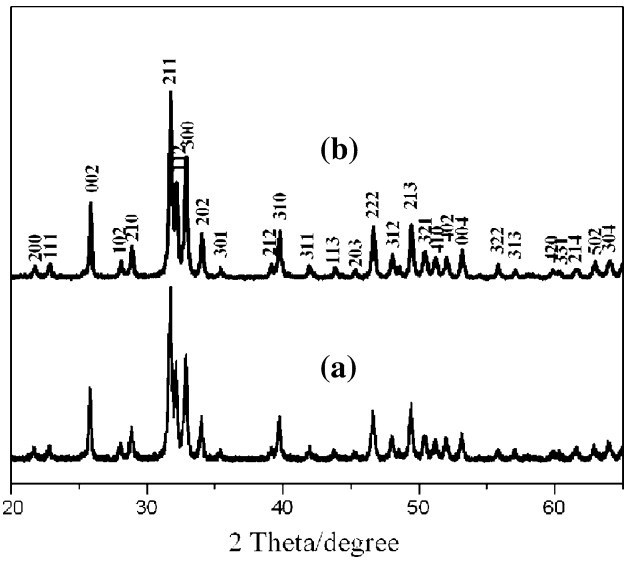

Fig. 1 XRD patterns of the HAP nanorods obtained (*a*) at 180 °C, (*b*) the HAP nanorods were calcined in 800 °C

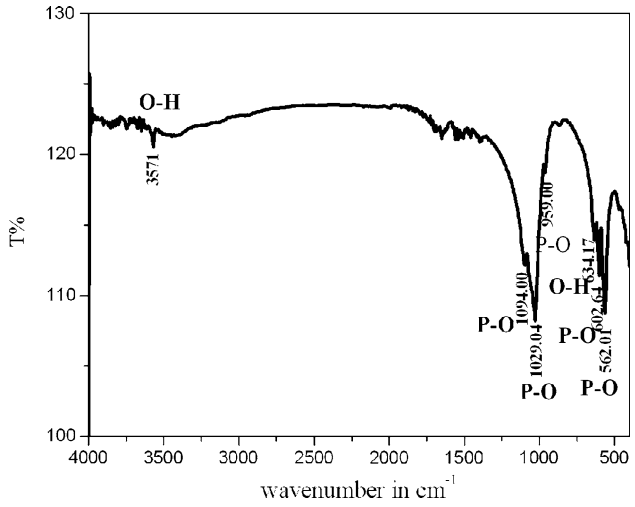

Fig. 2 FTIR spectrum of the calcium phosphate nanorods obtained with [PVP] = 1.36×10^{-4} mol L^{-1}, $[Ca^{2+}]/[HPO_4^{2-}] = 3/2$ at 180 °C

which indicates the high stability of the HAP nanorods (Fig. 1b).

Figure 2 shows the FT-IR spectrum of the nanorods with the characteristic phosphate absorption bands at ca. 1094, 1029, 959, 602, and 562 cm^{-1}. The broad peaks for inorganic phosphate at 1020–1100 cm^{-1} assign to υ_3 PO_4 antisymmetric stretching, 959 and 634 cm^{-1} are υ_1 PO_4 antisymmetric stretching, 602 and 562 cm^{-1} are υ_4 PO_4 antisymmetric deformation. The spectrum also shows hydroxide absorption bands at about 634 and 3600 cm^{-1}, typically observed in a HAP FT-IR spectrum.

The TEM and SEM images of HAP nanorods obtained in typical synthesis are shown in Fig. 3, the nanorods have an average diameter of 20–25 nm and length up to several micrometers (Fig. 3a). The inset of Fig. 3b shows the enlarged SEM image of the HAP nanorods.

Further experiments were carried out to investigate the effect of various reaction conditions on the morphology and structure of the products. We found temperature is an important factor for the sample morphology (Fig. 4). At 140 °C, though the product was rod-like, its length and diameter were not uniform, as shown in Fig. 4a. When the temperature increased to 160 °C, the nanorods became longer, and the diameter of the nanorods turned to be more uniform, a typical TEM image is presented in Fig. 4b. The uniform nanorods with diameter of 20–25 nm and length up to several micrometers could be obtained at a higher temperature (180 °C) (Fig. 4c). Further increasing the temperature to 220 °C did not lead to any increment in length, however, the samples began to congregate and short and thick nanoplates were obtained (Fig. 4d). The synthesis reaction is believed to be an endothermic reaction, the reaction and Ostwald ripening were incomplete at 140 °C, hence, the products with bad-defined morphology were obtained. On the other hand, when the temperature was too high (i.e. 220 °C), the nanorods tended to congregate in order to decrease surface energy, that resulted in the formation of thick and asymmetrical nanorods.

From the experiment, we find the morphologies of the HAP nanocrystals can be improved by the hydrothermal treatment observably.

The TEM images of the HAP nanocrystals obtained with different PVP concentration are shown in Fig. 5. Figure 5a is the TEM micrograph of the synthesized HAP powders without PVP. It is clear that the product consists of two kinds of particles. The typical one is rod-like, which is at least 200 nm in length and has an aspect ratio of 10 or more, and is not prevailing in quantity. Instead, numerous immature particles are found. Although the immature particles have a tendency to preferentially grow along one direction they are not classified as rod-like particles in this

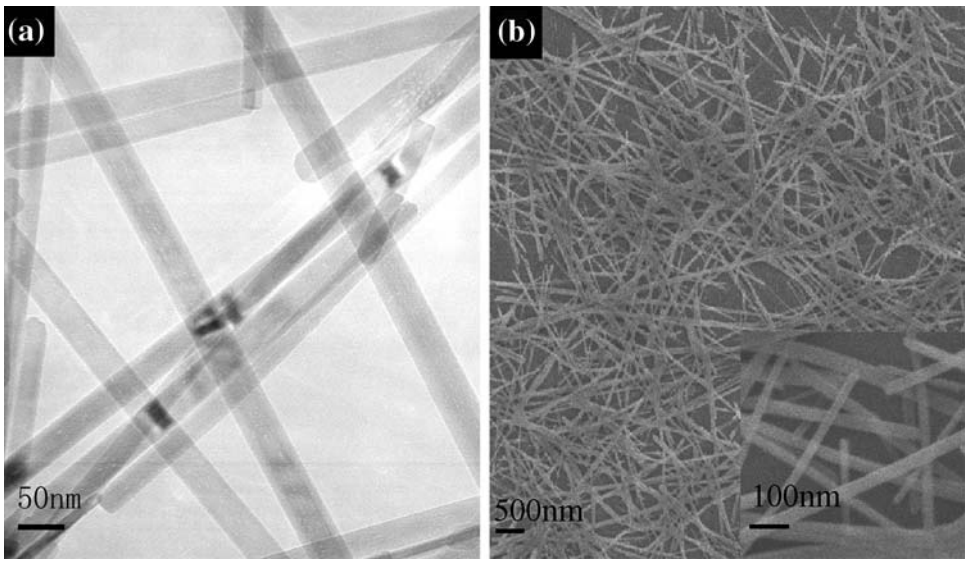

Fig. 3 **a** TEM and **b** SEM images of HAP nanorods, the inset in **b** shows the nanorods enlarged image

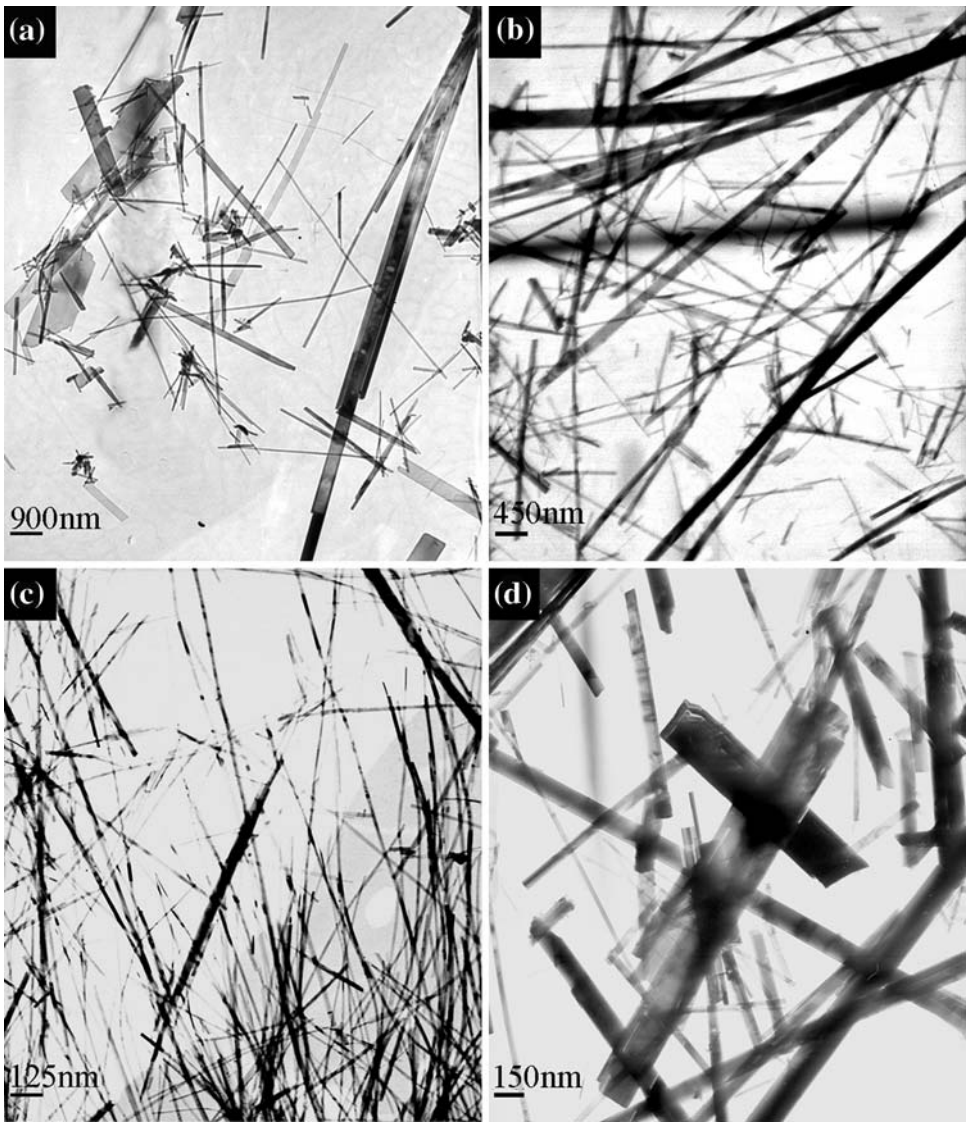

Fig. 4 TEM micrographs of HAP obtained with different hydrothermal treatment temperatures for 24 h. ($[Ca^{2+}]/[HPO_4^{2-}] = 3/2$, $[PVP] = 1.36 \times 10^{-4}$ mol L^{-1}, pH = 6–7) **a** 140 °C, **b** 160 °C, **c** 180 °C, **d** 220 °C

paper. When the concentration of PVP increased to 0.91×10^{-4} mol L^{-1}, the TEM micrograph of the synthesized HAP powders was shown in Fig. 5b. Although some immature particles could still be observed, the number of them is far less than that in Fig. 5a. Meanwhile, the typical size of the rod-like particles in Fig. 5b is found to be larger than that in Fig. 5a. Further increasing the concentration of PVP to 1.36×10^{-4} mol L^{-1}, except for some rod-like particles of about 400 nm in length, the typical size of the rod-like particles in Fig. 4c is 20–25 nm in diameter and several micrometers in length. Hence, uniform HAP nanorods can be obtained at 1.36×10^{-4} mol L^{-1}. Because HAP nanorods could still form without the presence of PVP, the formation of the rod-like morphology should be resulted from the growth habit of HAP along the c-axis. But the particles in Fig. 4c exhibited a rod-like morphology with a higher aspect ratio, which indicated that PVP greatly facilitated the formation of HAP nanorods with a high aspect ratio. The exact role of PVP is supposed that it has similar effect as the collagen matrix in the biomineralization process does, i.e., it acts as a surface-regulating polymer to result in the rod-like morphology of the HAP crystal. The role of PVP lies in the combination of two effects: (1) spatial effect, and (2) electrostatic and hydrogen bond effects. PVP has a polyvinyl skeleton with polar group, the N–C=O group in PVP maybe preferentially adsorb on the faces parallel to the (001) axis direction of HAP nanocrystal, leading to preferential growth along the (001) direction, which is in favor of the directional growth of nanorods with high aspect ratio. Because the O–H groups

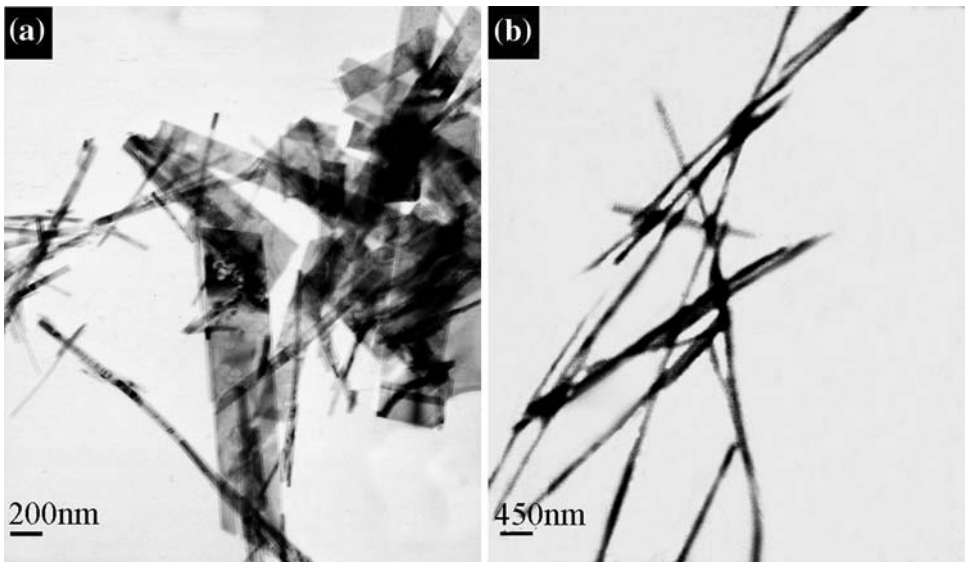

Fig. 5 TEM micrographs of HAP obtained with hydrothermal treatment for 24 h at 180 °C, ($[Ca^{2+}]/[HPO_4^{2-}] = 3/2$, pH = 6–7) **a** [PVP] = 0 mol L^{-1}, **b** [PVP] = 0.91×10^{-4} mol L^{-1}

are abundantly located on the surface of HAP crystal, the hydrogen bond will be formed between PVP and HAP, which prevent the aggregation of the nanorods and the growth along the direction vertical to the c-axis [23]. Therefore, in a low concentration of PVP solution, little of immature nanorods could be still found.

Figure 6 shows the morphologies of the HAP nanocrystals obtained with different molar ratios of $Ca(NO_3)_2$ to Na_2HPO_4. When the molar ratio was kept at 1/2, a mass of short rod-like nanocrystals was obtained (Fig. 6a). Generally increasing the molar ratio, the length of the rod-like nanocrystals also increased (Figs. 4c). But further increment of the molar ratio to 2/1 resulted in the decrease in length with relatively less effect on the diameter (Fig. 6b). In our experiment, we found that when the molar ratio varied between 1/2 and 3/2, not only the length of the sample increased, but also the sample turned to pure HAP. At a low molar ratio, excessive Na_2HPO_4 not only eliminates HNO_3 as by-product of the synthesis but also hydrolyzes to form NaOH. NaOH is known to disfavor the anisotropic growth [24] and could selectively adsorb on certain crystal surfaces, hence resulted in the formation of short nanorods. By increasing the molar ratio, the amount of NaOH gradually decreased and the length of the rods increased accordingly. When the molar ratio reached 3/2, surplus of Na_2HPO_4 could be eliminated by HNO_3 and no NaOH was formed, so the uniform HAP nanorods were obtained. Further increasing the molar ratio to 2/1, HAP

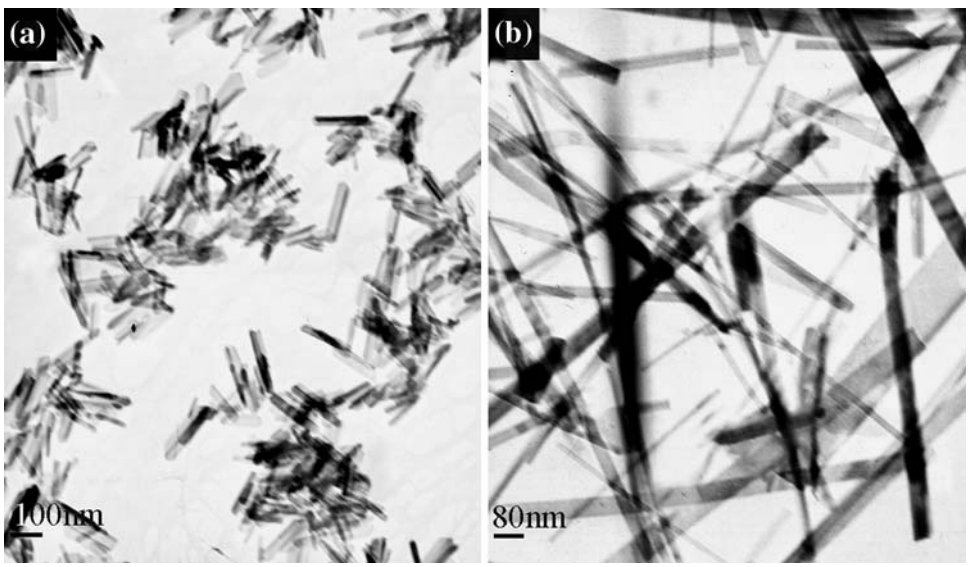

Fig. 6 TEM micrographs of HAP obtained with hydrothermal treatment for 24 h at 180 °C, ([PVP] = 1.36×10^{-4} mol L^{-1}, pH = 6–7) **a** $[Ca^{2+}]/[HPO_4^{2-}] = 1/2$, **b** $[Ca^{2+}]/[HPO_4^{2-}] = 2/1$

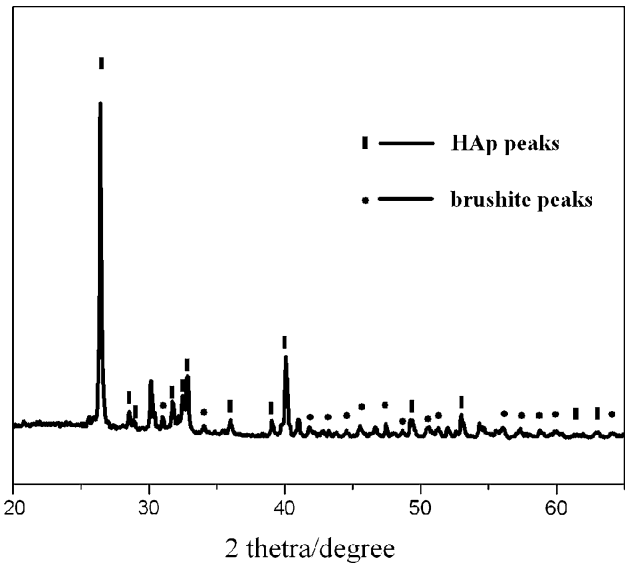

Fig. 7 The XRD pattern of HAP obtained with $[Ca^{2+}]/[HPO_4^{2-}] = 2/1$ hydrothermal treatment to 180 °C for 24 h

and brushite ($CaHPO_4{\cdot}2H_2O$) were formed as final products and the XRD pattern of the product is presented in Fig. 7. The synthesis of the sample is based on the following reaction:

$$Na_2HPO_4 + Ca(NO_3)_2 + 2H_2O \rightarrow CaHPO_4{\cdot}2H_2O + 2NaNO_3 \quad \text{(at room temperature)} \quad (1)$$

$$4Ca(NO_3)_2 + 6CaHPO_4{\cdot}2H_2O \rightarrow Ca_{10}(PO_4)_6(OH)_2 + 8HNO_3 + 10H_2O \quad \text{(during hydrothermal route)} \quad (2)$$

The anisotropic growth of the product may result in the morphology change.

Hydrothermal treatment time was another factor that affected the product morphology. As shown in Fig. 8, when the treatment time was 8 h (Fig. 8a), the length and the diameter of the nanorods obtained were not uniform. As reaction time prolonged, the length of the nanorods significantly increased, whereas the diameter decreased. Optimal reaction time was found to be 24 h, long and thin HAP nanorods were obtained (Fig. 4c). Further increasing the reaction time resulted in the decrease of length and formation of thick rods (Fig. 8b). In our experiment, the transition of brushite into HAP was affected by hydrothermal treatment time. When the time was too short, the reaction 2 was incomplete, so the final sample contained both brushite and HAP, the morphology of which was bad defined. As reaction time increased, the purity and uniformity of HAP nanorods were improved. On lengthening the time to 48 h, the lateral capillary forces along the length of a nanorod became higher, compared with the width, hence forcing the side-by-side alignment of nanorods to thick rods [25].

The typical experimental parameters and representative results mentioned above are listed in Table 1.

With a view to obtain a more comprehensive understanding of the structure transformation and morphology evolution of the HAP nanocrystals, the calcium phosphate system represents one of the most complex families of materials due to the existence of a number of phosphate compounds. Furthermore, the stability of each phosphate is affected by not only small compositional changes but also the reaction conditions including the solvent, precursors, temperature, time, pressure, pH value, and the complexing

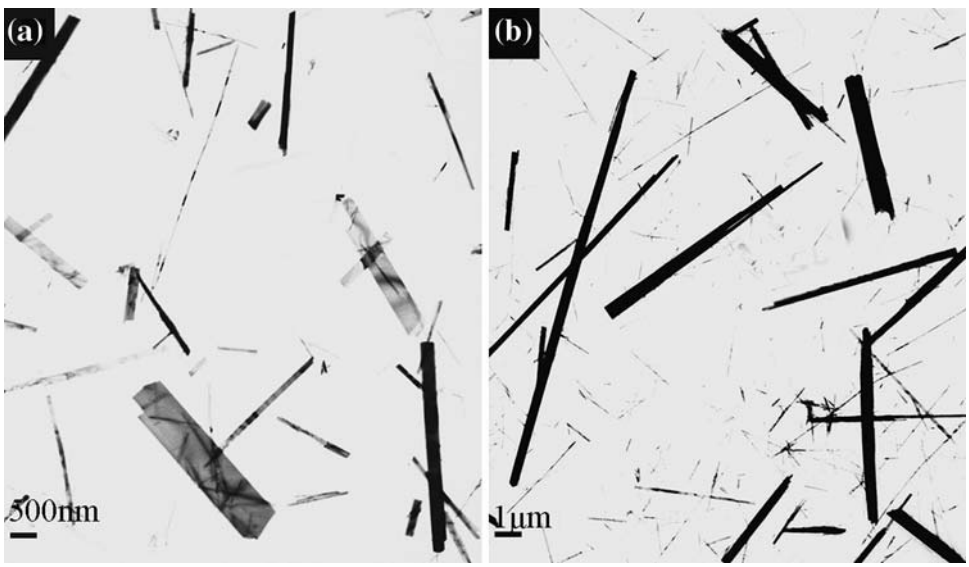

Fig. 8 TEM images of HAP samples obtained at 180 °C, $[Ca^{2+}]/[HPO_4^{2-}] = 3/2$, $[PVP] = 1.36 \times 10^{-4}$ mol L^{-1}, with hydrothermal treatment for **a** 8 h, **b** 48 h

Table 1 The experimental parameters and representative results obtained under different reaction conditions

PVP/ ($*10^{-4}$M)	Ca^{2+}/ HPO_4^{2-}	T (°C)	t (h)	Product morphology
2.5	1/1	140	24	Non-uniform nanorods
2.5	1/1	160	24	More uniform nanorods
2.5	1/1	180	24	Uniform nanorods
2.5	1/1	220	24	Nanorods + nanoplates
0	1/1	180	24	Nanorods + nanoparticles
0.91	1/1	180	24	Nanorods (main)
1.36	1/1	180	24	Nanorods
2.5	1/2	180	24	Short nanorods
2.5	3/2	180	24	Short nanorods
2.5	2/1	180	24	Brushite occurred
2.5	1/1	180	24	Non-uniform nanorods
2.5	1/1	180	24	Thick nanorods

agents used for controlling the reaction kinetics [26]. The possible growth procedure of the HAP nanorods in our experiment is described as follows: in the beginning, when the as-obtained $Ca(NO_3)_2$ and Na_2HPO_4 solutions were mixed, reaction 1 occurred. An amorphous precursor phase, brushite with a Ca/P molar ratio of unity, was obtained. During hydrothermal treatment, solution-mediated crystal growth and phase transformation occurred, then HAP crystal nuclei formed. The synthesis of HAP nanoparticles was based on reaction 2, and Ca/P ratio of 1.5 was used for the reaction. Taking into account the HAP lattice constants ($a = 0.9400$ Å and $c = 6.930$ Å) and the hexagonal symmetry with the space group $P63/m$, its unit cell will be arranged along the c-axis. The growth habit of HAP along the c-axis can be found from Fig. 5a without PVP, which has also been proved by the previous work. When HAP nucleated from the solution, the growth habit emerged simultaneously. PVP in the solution will greatly prompt this growth habit. During the growing process, PVP can be desorbed into water because of the unstable surface adsorption. Along with desorption of PVP, the crystal growth is corporately controlled by Ostwald ripening and oriented attachment process. Followed by increasing hydrothermal treatment time, the HAP crystal nuclei stacked into well-organized arrays up to nanometers in dimension, long HAP nanorods were obtained after 24 h. However, prolonged treatment time resulted in the formation of thick nanorods.

Conclusion

In summary, we have successfully prepared pure HAP nanorods using a simple and mild hydrothermal treatment method in the presence of PVP under near neutral condition. In the crystallization process, the oriented attachment and the effect of PVP were vital for the regulation of the nucleation and crystal growth of rod-like HAP crystal. The formation behavior mechanism is introduced to explain the great tendency of HAP crystal to preferentially grow along the c-axis direction. The reaction temperature, molar ratio of Ca^{2+} to HPO_4^{2-}, and hydrothermal treatment time are also critical toward obtaining controlled morphology and grain size of HAP crystals. We believe that the HAP nanorods might have abroad application in the field of biological and medicine.

Acknowledgements We thank the National Natural Science Foundation of China (20573017) and Analysis and Testing Foundation of Northeast Normal University for financial supporting.

References

1. Armstrong G, Armstrong AR, Canales J, Bruce PG (2005) Chem Commun 19:2454
2. Song RQ, Xu AW, Yu SH (2007) J Am Chem Soc 129:4152
3. Dong LH, Chu Y, Sun WD (2008) Chem Eur J 14:5064
4. Martin BR, Dermody DJ, Reiss BD, Fang MM, Lyon LA, Natan MJ, Mallouk TE (1999) Adv Mater 11:1021
5. Govindaraj A, Satishkumar BC, Nath M, Rao CNR (2000) Chem Mater 12:202
6. Jana NR, Gearheart L, Murphy CJ (2001) J Phys Chem B 105:4065
7. Xiao ZL, Han CY, Welp U, Wang HH, Kwok WK, Willing GA, Hiller JM, Cook RE, Miller DJ, Crabtree GW (2002) Nano Lett 2:1293
8. Pileni MP (2003) Nat Mater 2:145
9. Althues H, Kaskel S (2002) Langmuir 18:7428
10. Narayan KR, Anderson MT, Brinker CJ (1996) Chem Mater 8:1682
11. Burda C, Chen X, Narayanan R (2005) Chem Rev 105:1025
12. Hu J, Odom TW, Lieber CM (1999) Acc Chem Res 32:435
13. Yamashita Y, Uchida A, Yamakawa T, Shinto Y, Araki N, Kato K (1998) Int Orthop 22:247
14. Paul W, Sharma CP (1999) J Mater Sci Mater Med 10:383
15. Ito A, Nakamura S, Aoki H, Akao M, Teraoka K, Tsutsumi S, Onuma K, Tateishi T (1996) J Cryst Growth 163:311
16. Ioku K, Yoshimura M, Sōmiya S (1990) Biomaterials 1:57
17. Ahn ES, Gleason NJ, Nakahira A, Ying JY (2001) Nano Lett 1:149
18. Wu YJ, Bose S (2005) Langmuir 21:3232
19. Spanos N, Patis A, Kanellopoulou D, Andritsos N, Koutsoukos PG (2007) Cryst Growth Des 7:25
20. Sadasivan S, Khushalani D, Mann S (2005) Chem Mater 17:2765
21. Yao J, Tjandra W, Chen YZ, Tam KC, Mab J, Soh B (2003) J Mater Chem 13:3053
22. Cao MH, Wang YH, Guo CX, Qi YJ, Hu CW (2004) Langmuir 20:4784
23. Zhang YJ, Lu JJ (2008) Cryst Growth Des 8:2101
24. Liu JP, Huang XT, Li YY, Sulieman KM, He X, Sun FL (2006) J Mater Chem 16:4427
25. Kwan S, Kim F, Akana J, Yang P (2001) Chem Commun 5:447
26. Kumta PN, Sfeir C, Lee D-H, Olton D, Choi D (2005) Acta Biomater 1:65